

April 15, 1991

Zero magnetic-field ferromagnetic-resonance properties of single-crystal YIG/GGG/YIG layers

K. Sun

P. Dorsey

C. Vittoria
Northeastern University

Recommended Citation

Sun, K.; Dorsey, P.; and Vittoria, C., "Zero magnetic-field ferromagnetic-resonance properties of single-crystal YIG/GGG/YIG layers" (1991). *Electrical and Computer Engineering Faculty Publications*. Paper 137. <http://hdl.handle.net/2047/d20002308>



Zero magnetic field ferromagnetic resonance properties of singlecrystal YIG/GGG/YIG layers

K. Sun, P. Dorsey, and C. Vittoria

Citation: *J. Appl. Phys.* **69**, 6212 (1991); doi: 10.1063/1.348811

View online: <http://dx.doi.org/10.1063/1.348811>

View Table of Contents: <http://jap.aip.org/resource/1/JAPIAU/v69/i8>

Published by the [American Institute of Physics](#).

Related Articles

Optically driven method for magnetically levitating diamagnetic material using photothermal effect

J. Appl. Phys. **111**, 023909 (2012)

Simultaneous observation of magnetostatic backward volume waves and surface waves in single crystal barium ferrite platelets with in-plane easy axis

J. Appl. Phys. **111**, 023901 (2012)

The effect of Fe²⁺ ions on dielectric and magnetic properties of Yb₃Fe₅O₁₂ ceramics

J. Appl. Phys. **111**, 014112 (2012)

Direct observation of magnetic phase coexistence and magnetization reversal in a Gd_{0.67}Ca_{0.33}MnO₃ thin film

Appl. Phys. Lett. **100**, 022407 (2012)

Epitaxial thin films of p-type spinel ferrite grown by pulsed laser deposition

Appl. Phys. Lett. **99**, 242504 (2011)

Additional information on *J. Appl. Phys.*

Journal Homepage: <http://jap.aip.org/>

Journal Information: http://jap.aip.org/about/about_the_journal

Top downloads: http://jap.aip.org/features/most_downloaded

Information for Authors: <http://jap.aip.org/authors>

ADVERTISEMENT



Zero magnetic field ferromagnetic resonance properties of single-crystal YIG/GGG/YIG layers

K. Sun, P. Dorsey, and C. Vittoria

Department of Electrical and Computer Engineering, Northeastern University, Boston, Massachusetts 02115

This study is an extension of previous work dealing with single crystals of YIG/GGG/YIG grown in (110) layers. Ferromagnetic resonance (FMR) measurements for fields along the $\langle 111 \rangle$ axis were performed. The microwave measurements reveal hysteretic behavior as the FMR frequency is measured for positive and negative magnetic fields H . For H in which the magnetic moment is zero (spin flop) the FMR frequency goes through a discrete and measurable jump or change. This discontinuity in the FMR frequency at the spin-flop condition is attributed to the magnetostatic interaction between the two YIG layers.

I. INTRODUCTION

The successful development of magnetic multilayered structures has generated great interest in the microwave properties of these structures. In particular, the study of double-layered structures are of special interest,¹⁻⁶ since they are the simplest structure to consider from a production point of view as well as understanding their physical properties. In this paper, we report on the microwave resonance properties of a single-crystal layered structure of YIG/GGG/YIG/GGG, where YIG and GGG are the abbreviations for yttrium iron garnet and gadolinium gallium garnet, respectively. Ferromagnetic resonance (FMR) measurements for fields (near zero) along the $\langle 111 \rangle$ axis were performed. The microwave measurements revealed a hysteretic behavior as the FMR frequency is measured for positive and negative fields of H . At fields in which the moment is zero (spin flop) the FMR frequency goes through a discrete and measurable jump or change. We attribute this discontinuity in the FMR frequency at the spin-flop condition to the magnetostatic interaction between the two YIG layers.

II. EXPERIMENTAL RESULTS

The geometry of the double-layered YIG structure and angular orientations of the two magnetizations of the two YIG layers M_1 and M_2 , and the applied dc field H_a are shown in Fig. 1, where a paramagnetic GGG film of thickness ($d_2 = 1 \mu\text{m}$) is placed between two YIG films, and the GGG substrate (d_4) is assumed to be infinitely thick. The capital letters refer to the crystal axes while (ϕ, β) , (ϕ_1, θ_1) , and (ϕ_2, θ_2) refer to the angular distributions of H_a , M_1 , and M_2 , respectively. The thicknesses (d_1, d_3) of the two YIG layers were about $1 \mu\text{m}$ while the diameter of the sample was 5 mm.

The ferromagnetic resonance (FMR) measurements were performed by using a microwave cavity operating at 9.5 GHz to measure the physical parameters of the layered films. The physical parameters used in this study are from a previous work.¹ For the layer next to the GGG substrate (layer 1), we have $4\pi M_{\text{eff}}^{(1)} = 1750 \text{ G}$, $2K_1^{(1)}/M = -82 \text{ Oe}$, $2K_u^{(1)}/M = 0$ and for the other layer (layer 2), we have $4\pi M_{\text{eff}}^{(2)} = 1256 \text{ G}$, $2K_1^{(2)}/M = -82 \text{ Oe}$,

$2K_u^{(2)}/M = 50 \text{ Oe}$, and $g = 2.025$, where $4\pi M_{\text{eff}}^{(i)}$ ($i=1,2$) is the sum of the saturation magnetization and any source of uniaxial magnetic anisotropy field normal to the film plane.

In order to observe zero-field resonance, the sample was placed at the junction of a slot-coplanar device, the pattern of which is shown in Fig. 2. In the measurements, the frequency is swept while the applied dc field H is fixed. The fields decreased from positive, through zero to negative, and then reversed. For a given applied dc field, there existed two resonant signals, each of which corresponds to one layer of the single-crystal double-layered film. In order to attribute each resonance to its corresponding YIG layer, the top layer was mechanically polished. After each polishing step the FMR signal was recorded and compared with previous FMR results. A decrease in the magnitude of the resonant signal was attributed to the thinning of the YIG layer exposed to the free surface. It was found that in the measurements the resonance corresponding to the layer between the GGG layers has a stronger absorption than the other YIG layer.

We have plotted the FMR frequency versus the applied field for the resonance line corresponding to the layer next to the GGG substrate in Fig. 3, where the applied field was along the $\langle 111 \rangle$ axis; circles and solid circles represent the applied fields varying from negative to positive and positive to negative, respectively. Figure 3 illustrates a microwave hysteretic behavior when the applied field is near $\pm 2 \text{ Oe}$. In order to compare microwave hysteretic behavior with the dc hysteretic behavior of the double-layered YIG structure, the hysteresis curve was obtained from a vibrating sample magnetometer (VSM) with the applied field also along the $\langle 111 \rangle$ axis (see Fig. 3). We found that for $H \sim 1.7 \text{ Oe}$ (spin flop) the FMR frequency goes through a discrete and measurable jump or change. Amplitude of the change is about 30 MHz. This discontinuity in the FMR frequency around the spin-flop condition can be explained in terms of the magnetostatic interaction between the two YIG layers.

III. ANALYSIS

The magnetostatic interaction energy between the two YIG layers is expressed by $C M_1 \cdot M_2$, where C is the coupling coefficient. Thus the total free magnetic potential en-

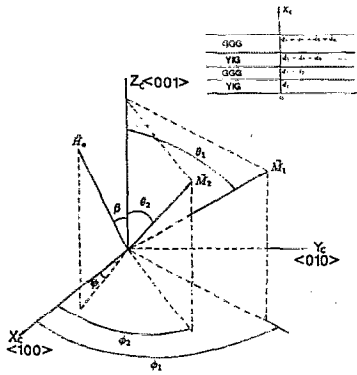


FIG. 1. A cross view of the geometrical configuration of the double-layered YIG film and orientation of the double-layered YIG film in relation to the angular parameters used for the calculations. The capital letters refer to the crystal axes while (ϕ, β) , (ϕ_1, θ_1) , and (ϕ_2, θ_2) refer to the angular distributions of H_0 , M_1 , and M_2 .

ergy of the whole structure is the sum of the free energy of each individual layer and the coupling energy as shown below:

$$F = F_1 + F_2 + CM_1 \cdot M_2, \quad (1)$$

where F_1 and F_2 are the free energies of layers 1 and 2, respectively. For the case of H in the $(1\bar{1}0)$ plane, the free potential energy of each layer is given¹ as

$$F_i = -HM_i[\cos \theta_i \cos \beta + \sin \theta_i \sin \beta \cos(\phi_i - \pi/4)] + \pi M_i^2[\sin^2 \theta_i(1 - \sin 2\phi_i)] + K_1^{(i)}[(3 - 4 \cos 2\theta_i + \cos 4\theta_i)(1 - \cos 4\phi_i)/8 + 1 - \cos 4\theta_i]/8 - K_u^{(i)} \cos^2(\theta_i - \alpha_i), \quad i=1,2, \quad (2)$$

where θ_i and ϕ_i are the polar and azimuthal angles of M_i and α_i is the angle between the easy axis of the in-plane anisotropy and the $[001]$ axis. In Eq. (2) the magnetizing, demagnetizing, cubic anisotropy $K_1^{(i)}$, and the in-plane-induced anisotropy $K_u^{(i)}$ energies are included with $i=1,2$ denoting the corresponding parameters for layers 1 and 2.

The resonant condition can be calculated from⁷

$$\left(\frac{\omega_i}{\gamma}\right)^2 = \frac{1}{M_i^2 \sin^2 \theta_i} \left[\frac{\partial^2 F}{\partial \theta_i^2} \frac{\partial^2 F}{\partial \phi_i^2} - \left(\frac{\partial^2 F}{\partial \theta_i \partial \phi_i} \right)^2 \right]_{\theta_i = \theta_{i0}, \phi_i = \phi_{i0}},$$

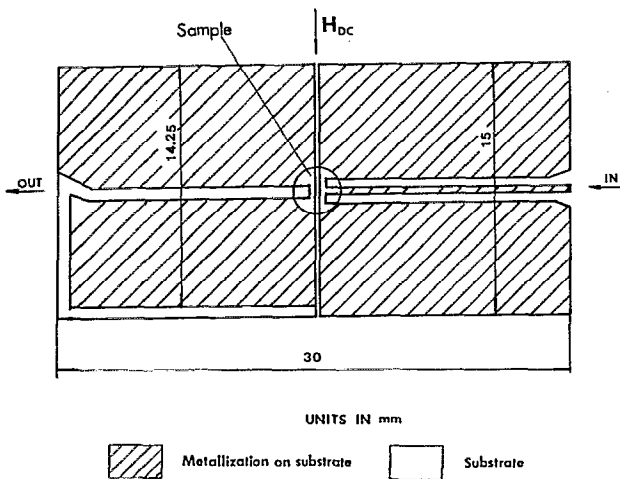


FIG. 2. The pattern of the slot-coplanar device. The sample is placed at the junction of the device.

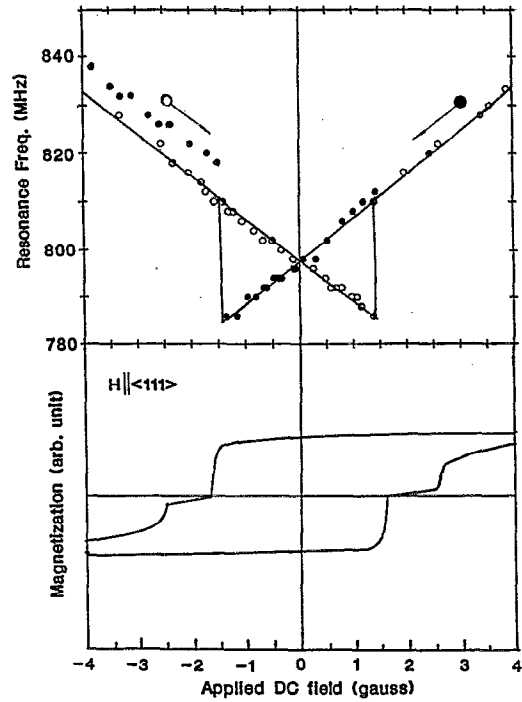


FIG. 3. FMR frequency vs applied field around zero field and comparison between microwave hysteretic behavior and static hysteresis curve. The applied field is along the $\langle 111 \rangle$ axis. Circles and solid circles represent the field varying from negative to positive value and from positive to negative value, respectively. The solid line in the plot of FMR frequency vs applied field is the calculated result.

$$i=1,2, \quad (3)$$

where $\gamma = g(e/2mc)$, θ_{i0} and ϕ_{i0} are the equilibrium angles at resonance, $\omega_i/2\pi$ is the operating frequency, and $\partial^2 F/\partial \theta_i^2$, $\partial^2 F/\partial \phi_i^2$, and $\partial^2 F/\partial \theta_i \partial \phi_i$ can be found in the Appendix.

From the equilibrium conditions we obtain

$$\frac{\partial F}{\partial \phi_i} = 0, \quad i=1,2, \quad (4)$$

$$\frac{\partial F}{\partial \theta_i} = 0, \quad i=1,2. \quad (5)$$

Solving these equations results in the equilibrium angle $\phi_i = 45^\circ$ which means that both M_1 and M_2 lie in the film plane for all angles of $H(\beta)$ in the plane. Since the two equations of Eq. (5) include θ_1 , θ_2 and the coupling coefficient C ($\phi_{10} = \phi_{20} = 45^\circ$), another equation must be supplemented such that the complete solution can be obtained. It is noted from static hysteresis measurements (VSM) that the hysteresis loop relates the total magnetization of the two YIG layers to the orientations $(\theta_1, \phi_1, \theta_2, \phi_2)$ of the two static magnetizations. For a given value of dc field, the measured total magnetization can be represented as

$$M_{\text{meas}} = M_s[\cos(\beta - \theta_1) + \cos(\beta - \theta_2)]. \quad (6)$$

In this study, we are interested in zero-field properties, in particular properties at the spin-flop condition ($M_{\text{meas}} = 0$). At the spin-flop condition ($H \approx 1.7$ Oe), C is

found to be 0.075. This value was used to compute the FMR frequency around zero field. The calculated result is represented by the solid line which is shown in Fig. 3. It is seen that a good agreement was obtained between the experimental and calculated results. However, the measured FMR frequency in Fig. 3 is not symmetrical about zero field. This nonsymmetry may be due to demagnetizing fields of the irregular-shaped sample.

In summary, we have studied the zero-field properties of a single-crystal layered structure of YIG/GGG/YIG/GGG. Ferromagnetic resonance (FMR) measurements for fields (near zero) along the $\langle 111 \rangle$ axis were performed. The microwave measurements reveal a hysteretic behavior as the FMR frequency is measured for positive and negative field values. For $H \sim 1.7$ Oe (spin flop) the FMR frequency goes through a discrete and measurable jump or change. This discontinuity in the FMR frequency at the spin-flop condition is due to the magnetostatic interaction between the two YIG layers. The source of this magnetostatic field is most likely due to edges.

ACKNOWLEDGMENTS

We wish to thank ONR for supporting the research in part. Also, we thank Dr. H. L. Glass, Dr. P. De Gasperis, and Dr. R. Marcelli for useful discussions in this work.

APPENDIX

For $\phi_1 = \phi_2 = 45^\circ$, we have

$$\frac{\partial^2 F}{\partial \theta_i^2} = HM_i \cos(\theta_i - \beta) + \frac{K_1^i}{2} (\cos 2\theta_i + 3 \cos 4\theta_i) + 2K_u^i \cos 2\theta_i - CM_1 M_2 \cos(\theta_1 - \theta_2)$$

and

$$\frac{\partial^2 F}{\partial \phi_i^2} = HM_i \sin \theta_i \sin \beta + 4\pi M_i^2 \sin^2 \theta_i - \frac{K_1^i}{4} (3 - 4 \cos 2\theta_i + \cos 4\theta_i) - CM_1 M_2 \sin \theta_1 \sin \theta_2,$$

$$\frac{\partial^2 F}{\partial \theta_i \partial \phi_i} = 2\pi M_i^2 \sin 2\theta_i.$$

- ¹K. Sun, C. Vittoria, H. L. Glass, P. De Gasperis, and R. Marcelli, *J. Appl. Phys.* **67**, 3088 (1990).
- ²P. Grünberg, *J. Appl. Phys.* **57**, 3673 (1985).
- ³L. L. Hinchey and D. L. Mills, *Appl. Phys.* **57**, 3687 (1985).
- ⁴J. J. Krebs, C. Vittoria, B. T. Jonker, and G. A. Prinz, *J. Magn. Magn. Mater.* **54-57**, 811 (1986).
- ⁵P. Grünberg, P. Schreiber, Y. Pang, U. Walz, M. B. Brodsky, and H. Sowers, *J. Appl. Phys.* **61**, 3750 (1987).
- ⁶J. J. Krebs, P. Lubitz, A. Chaiken, and G. A. Prinz, *Phys. Rev. Lett.* **63**, 1645 (1989).
- ⁷J. Smit and H. G. Beljers, *Philips Res. Rep.* **10**, 113 (1959).